Ibrahim et al. Adv Metallurg Mater Eng 2017, 1(1):1-7
DOI: 10.36959/508/392 | Volume 1 | Issue 1

Advances in Metallurgical and Material Engineering

Research Article Open Access

"Mechanical and *In Vitro* Corrosion Properties of a Heat-Treated Mg-Zn-Ca-Mn Alloy as a Potential Bioresorbable Material"

Hamdy Ibrahim[1], N Shayesteh Moghaddam[1] and Mohammad Elahinia[2]*

[1]Graduate Student, Department of Mechanical Industrial and Manufacturing Engineering, University of Toledo, USA
[2]Professor, Department of Mechanical Industrial and Manufacturing Engineering, University of Toledo, USA

Abstract

Heat treatment is a practical approach that has been thoroughly studied to strengthen Mg alloys for different applications. The aim of this work is to study the effect of the addition of Mn and a heat treatment process on the mechanical and *in vitro* corrosion properties of a Mg-Zn-Ca-based alloy. The microstructure of the prepared Mg-1.2Zn-0.5Ca (wt.%) and Mg-1.2Zn-0.5Ca (wt.%) alloys, as-cast and heat-treated, was investigated using optical microscopy, scanning electron microscopy (SEM), energy dispersive spectroscopy (EDS). The mechanical properties of the prepared alloys were determined using microhardness, compression and tensile tests. *In vitro* immersion and potentiodynamic polarization (PDP) tests were used to assess the corrosion behavior of the alloys. It was found that the performed heat treatment process significantly enhances the mechanical and *in vitro* corrosion properties of the Mg-1.2Zn-0.5Ca and the Mg-1.2Zn-0.5Ca-0.5Mn alloys due to significant microstructural changes. The addition of 0.5 wt.% Mn to the Mg-Zn-Ca-based alloy resulted in a better age hardening response by increasing the mechanical strength and reducing the corrosion rate. Such heat-treated Mg-1.2Zn-0.5Ca-0.5Mn alloy is a good candidate for developing biocompatible bone fixation devices.

Keywords

Bone implants, Magnesium alloy, Heat treatment, Immersion test, Mechanical properties

Introduction

The commonly available technique for bone reconstructive surgeries is the use of metallic implants to immobilize bone in place for the completion of the healing process [1]. These metallic implants usually stay permanently in the body after the healing period which causes many problems such as stress shielding and possible irritation in the adjacent soft tissue [2]. Stainless steel (316L SS), surgical grade 5 titanium (Ti-6Al-4V) and CrCoMo are the most common materials being used for metallic implants since they offer high strength, durability and biocompatibility [3]. These materials present high stiffness (e.g., ~193 GPa for 316L SS, ~116 GPa for Ti-6Al-4V, ~220 GPa for CrCoMo) compared to that of cortical bone (5-23 GPa for cortical bone). Although the high stiffness is required for initial bone healing, over time, the abnormal stress distribution between the implants and bone may lead to implant breakage or bone loss around the implant (*i.e.,* stress shielding) [2]. It is therefore promising to utilize a fixation hardware which ensures enough immobilization as well as normal stress distribution during bone healing, then gradually starts to resorb once the bone is healed [2,4,5]. Magnesium (Mg), as a biodegradable metal in the body, is a proper candidate to be used for biomedical applications due to their low stiffness, high biocompatibility and high bioresorbability [2,6-9]. Several *in vivo* studies have confirmed the biocompatibility of different Mg alloying systems [7,9-12]. However, its low strength and rapid galvanic corrosion in physiological environments are the major concerns associated with commercially pure Mg [13]. However, it should be mentioned that ultrapure Mg has very slow corrosion rates which can be attributed to the absence of harmful impurities that promote galvanic corrosion [14]. One technique to enable the use of Mg in biomedical implants by alloying the Mg with other elements such as Al, Zn, Zr, Sr, Mn, Ca, Y and Rare earth elements (RE) [15-22]. However, one should carefully consider the toxicity of the degradation products to the body cells. As an example, the accumulation of Al in the body has been identified as a reason of hepatotoxicity and a possible reason for Alzheimer's disease [23-25]. In contrast, considering the level of resorption from an bioresorbable implant, Ca, Zn, Mn and Zr have been considered non-toxic to body since they can be absorbed from one's diet [13].

Mg-Zn-Ca-based alloys have recently attracted much attention to be used for orthopedic applications due to their biocompatibility and the possibility to tailoring their properties by post-fabrication processes (e.g. heat treatment) [22,26]. However, these alloys do not present sufficient strength that is required for holding fractured bones during the bone

***Corresponding author:** Mohammad Elahinia, Professor, Department of Mechanical Industrial and Manufacturing Engineering, University of Toledo, Toledo, OH 43606, USA, E-mail: mohammad.elahinia@utoledo.edu

Received: November 28, 2016; **Accepted:** February 07, 2017; **Published online:** February 10, 2017

Citation: Ibrahim H, Moghaddam NS, Elahinia M (2017) "Mechanical and *In Vitro* Corrosion Properties of a Heat-Treated Mg-Zn-Ca-Mn Alloy as a Potential Bioresorbable Material". Adv Metallurg Mater Eng 1(1):1-7

healing period (*i.e.*, 3-6 months). In addition to inherent low strength of Mg-Zn-Ca-based alloys, their fast degradation rate in the body plays an important role in further reducing their strength [20,27-29]. To this end, different techniques have been introduced to enhance mechanical and corrosion properties of these alloys including the addition of more alloying elements such as Mn and Zr [22,30,31], mechanical treatments such as extrusion and rolling, and heat treatments such as annealing and age hardening [26,27,32-34].

The addition of Mn to different Mg alloys was found to be a useful technique to improve the mechanical and corrosion properties by incorporating essentially insoluble metallic impurities such as Fe and Ni into harmless inter metallic phases [2]. Also, [22] showed that the addition of 0.5 wt.% of Mn to ternary Mg-Zn-Ca-based alloys was found to improve the mechanical properties and corrosion resistance by decreasing the grain size.

In general, heat treatment processes are more feasible than mechanical treatment when the part is fabricated into its final shape. With appropriate heat treatment for Mg-Zn-Ca-based alloys, fine and uniform inter metallic precipitation of secondary phases (mainly $Ca_2Mg_6Zn_3$) can be evolved within the α-Mg primary phase matrix which is the main reason for the mechanical properties enhancement [27,35-37]. Few studies focused on the effect of the heat treatment on the biocorrosion properties of Mg-Zn-Ca-based alloys. Lu Bradshaw, et al. [38] reported slower rate of biocorrosion after subsequent solution treatment and quenching on Mg-3Zn-0.3Ca (wt.%) alloy. Ji Parker, et al. [39] also demonstrated an enhancement in the biocorrosion resistance and biocompatibility of the heat treated Mg-35Zn-3Ca (wt.%) alloy. For quaternary Mg-Zn-Ca-Mn alloys, only one recent study investigated the microstructural and the mechanical properties of as-cast and heat-treated Mg-Zn-Ca-Mn alloys [40]. However, there is limited data in the literature on the heat treatment influence on the biocorrosion properties of a quaternary Mg-Zn-Ca-Mn alloy.

In this work, we aimed to study the effect of a heat treatment process (*i.e.,* solution treatment, quenching and age hardening) on the properties of a ternary Mg-Zn-Ca alloy (Mn-free) compared to a quaternary Mg-Zn-Ca-Mn alloy from microstructural, mechanical and biocorrosion perspectives. To this end, the ratio of Mn within the alloy composition and the heat treatment process parameter were carefully chosen in a way to achieve the optimum enhancement in the mechanical and corrosion properties.

Experimental Methods

Mg alloys preparation

The chemical composition of the Mg-Zn-Ca-based alloys which can lead to the optimum age hardening effect after the heat treatment process was carefully selected. For example, Ca and Zn contents are recommended to be less than 1 wt.% and 5 wt.%, respectively according to different studies in order to limit the excess formation of secondary phases which results in deteriorated mechanical and/or corrosion properties [15,29,31,41]. And since the range of 1.2 to 2.0 has been recommended for the Zn/Ca atomic ratio for an optimum heat treatment response [15,27,42,43] the Ca and Zn contents were chosen to be 0.5 wt.% and 1.2 wt.%, respectively. Finally, the addition of 0.5 wt.% Mn is proposed in this work to study its effect on the mechanical and corrosion behavior of the as-cast and heat-treated alloy. To this end, the Mg-1.2Zn-0.5Ca (wt.%) and Mg-1.2Zn-0.5Ca-0.5Mn (wt.%) alloys were designed and prepared.

The casting was conducted using commercially pure Mg, pure Zn, a 15% Ca-Mg master alloy, and $MnCo_3$. The melting was performed under a CO_2 + 0.5% SF6 protective gas atmosphere situation in a steel crucible. The melt was then cast into a steel permanent mold, started at room temperature. Finally, cylindrical ingots were produced.

To assure the melting of secondary phases (*i.e.,* Mg_2Ca and $Ca_2Mg_6Zn_3$) in the primary α-Mg matrix during the heat treatment process, the as-cast alloys (Mg-1.2Zn-0.5Ca and Mg-1.2Zn-0.5Ca-0.5Mn) were solution-treated in an inert gas environment using a tube furnace at 510 ˚C for 3 hours. The solution-treated alloy samples were then quickly cooled by quenching in water. Afterwards, an artificial age-hardening process was performed on the quenched alloy in an oil bath at 200 ˚C for 3 hours [27,32,33,34].

Characterizations

In this study, the microstructural, mechanical and corrosion properties of the as-cast and the heat-treated alloy samples were evaluated.

Microstructure investigation: The preparation of the microstructure samples started by mounting the as-cast and heat-treated alloy samples in polymeric material and then polishing using 180 to 2000 grit SiC papers in 90˚ parallel lines. The samples were subsequently polished using a Leco (St. Joseph, Michigan) imperial cloth pad with silica powder (0.05 μm) until a mirror surface was obtained. In the next step, the samples were etched in acetic glycol solution then quickly rinsed by water and wiped. Then, the samples were immersed in ethanol and ultrasonically cleaned for 3-5 min. Finally, the microstructure of the samples was characterized by conducting optical microscopy (using Meiji (Saitama, Japan) ML9430), scanning electron microscopy (SEM) and energy dispersive (EDS) analysis using Hitachi (Tokyo, Japan) S-4800.

Mechanical testing: In order to evaluate the mechanical properties of the as-cast and heat-treated alloys, the compressive and tensile tests were performed using an Instron-5569 universal testing machine at ambient temperature according to the ASTM E9-09 and the ASTM E8/E8M-15a standards, respectively. Moreover, the Vickers' hardness of the prepared samples was measured with a Clark micro hardness tester CM-400AT (Michigan, USA) using a 500 g load cell and 15 sec dwell time.

***In vitro* immersion test:** To prepare the samples for the *in vitro* corrosion investigation, coupons with diameter of 15 mm and thickness of 3 mm polished with 180 to 2000 grit SiC paper. The coupons were cleaned using ethanol and the weight of each coupon then was measured and recorded before the start of the immersion test. A simulated body fluid (SBF) medium was prepared according to the methods and chemical composition presented by [44].

The immersion test was conducted by submerging the polished and ethanol-degreased coupons in a glass reactor filled with SBF solution at pH 7.4 and 37 °C. To avoid localized pH increase in the vicinity of the samples, a continuous circulation of the SBF medium was achieved using a peristaltic pump [45]. The temperature was maintained at 37 °C by placing the system in an incubator during the test. In order to keep the pH in the range of 7.3 to 7.8 (physiological environment) during the test, a diluted hydrochloric acid (HCL) solution was regularly titrated into the SBF and the SBF solution was changed every 3 days. The test was performed for 14 days and the corrosion products were removed from the surface of the corroded samples before measuring their weights. By measuring the weight of each coupon before and after the test, the mass loss (mg/cm^2) was calculated using equation (1).

$$Mass\ Loss = \frac{m_i - m_f}{A} \quad (1)$$

Where m_i is the initial weight of coupon before immersion (mg), m_f is the final weight of each coupon after immersion (mg), A is the coupon's surface area exposed to the SBF solution (cm^2).

Potentiodynamic polarization (PDP) test: Polished coupons of the heat-treated Mg-1.2Zn-0.5Ca and Mg-1.2Zn-0.5Ca-0.5Mn alloys were molded into epoxy resin with only one side exposed (i.e., 1.77 cm^2) during the PDP test. A Gamry (Centennial, Colorado)

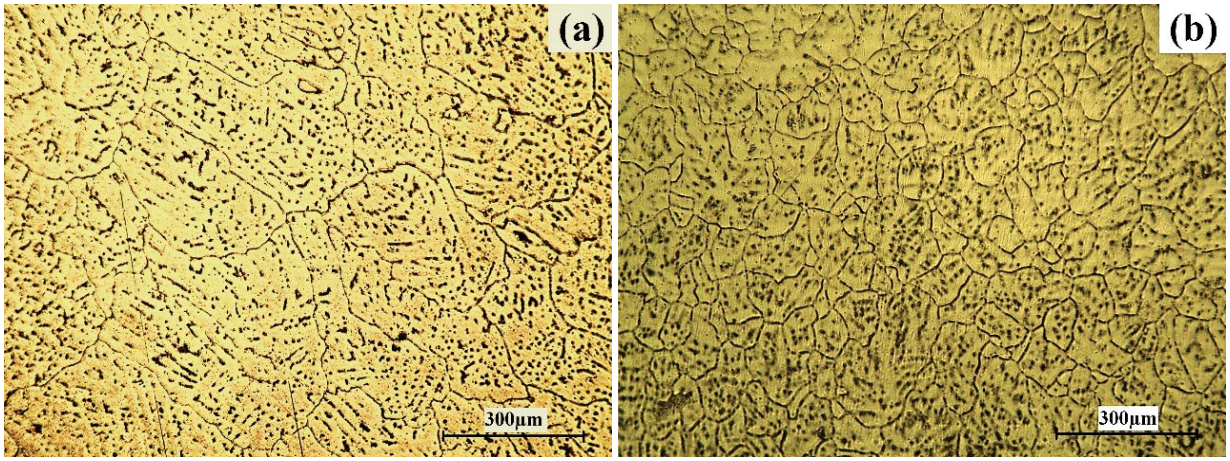

Figure 1: Optical micrographs of the as-cast a) Mg-1.2Zn-0.5Ca alloy; b) Mg-1.2Zn-0.5Ca-0.5Mn alloy.

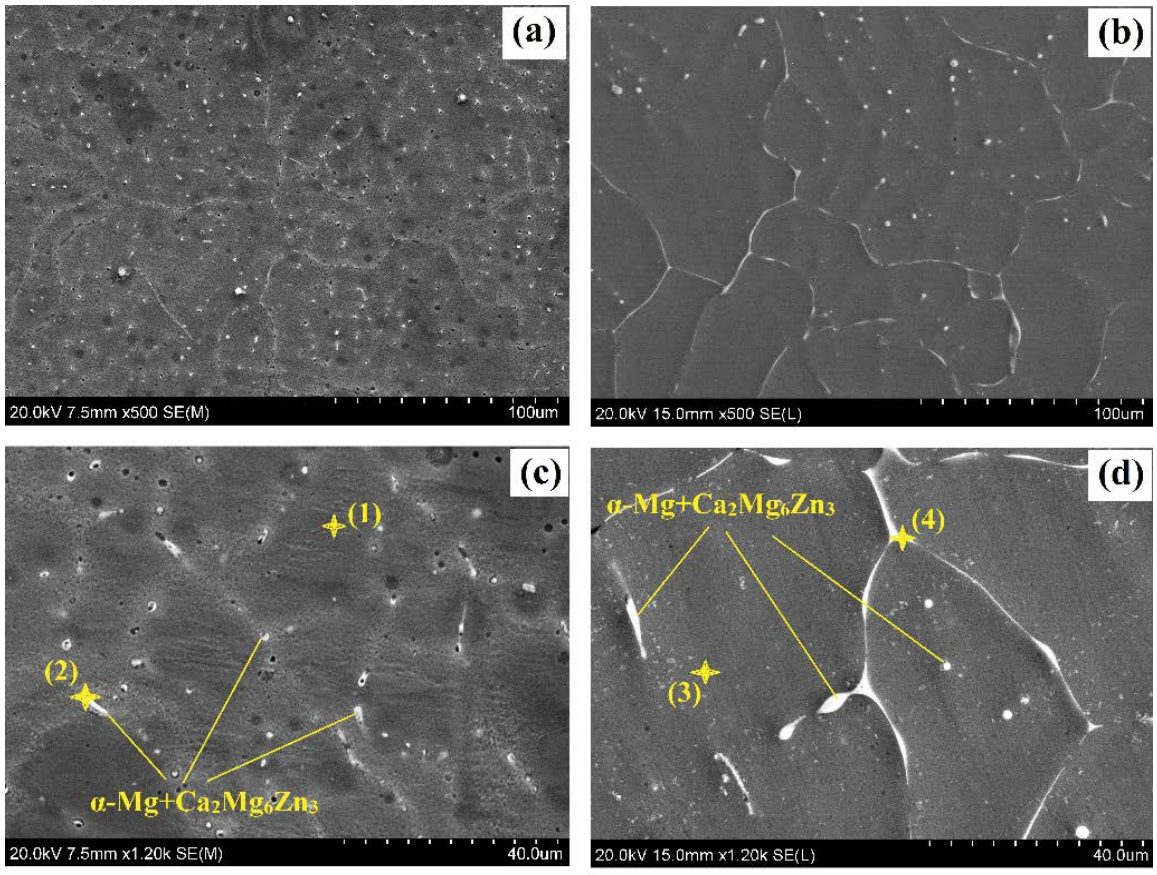

Point	Element wt. %			
	Mg	Zn	Ca	Mn
1	99.22	0.65	0.13	0.00
2	87.78	10.05	2.17	0.00
3	99.64	0.07	0.03	0.30
4	78.90	14.8	6.30	0.00

Figure 2: SEM micrographs and the corresponding EDS analysis of the as-cast (a), (c) Mg-1.2Zn-0.5Ca alloy, and (b), (d) Mg-1.2Zn-0.5Ca-0.5Mn alloy.

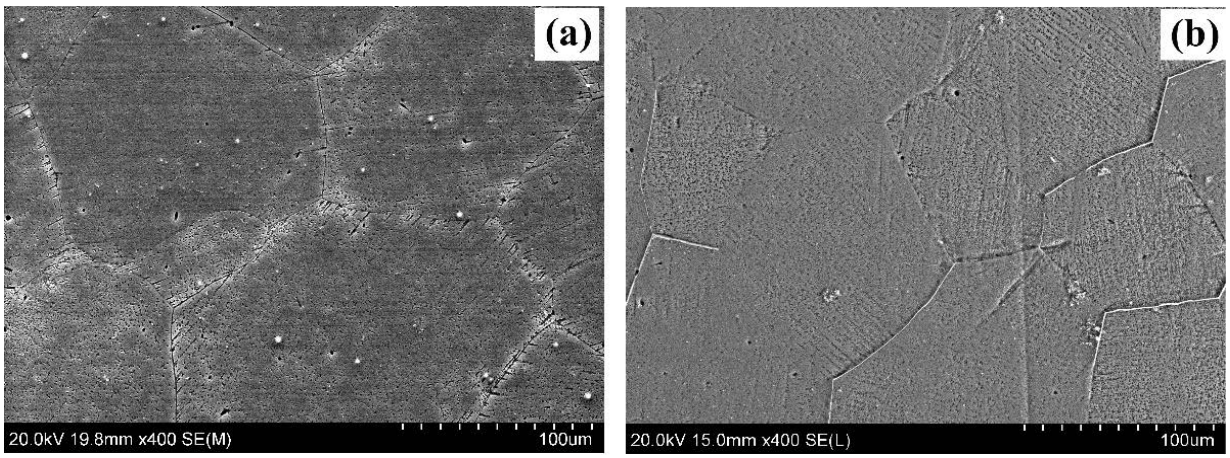

Figure 3: SEM micrographs of the heat-treated (a) Mg-1.2Zn-0.5Ca alloy; (b) Mg-1.2Zn-0.5Ca-0.5Mn alloy.

Table 1: Mechanical properties of the Mg-1.2Zn-0.5Ca and Mg-1.2Zn-0.5Ca-0.5Mn alloys, as-cast and heat-treated.

Alloy	Processing history	Micro-hardness (HV)	Compression properties			Tensile properties		
			Yield strength (MPa)	Ultimate strength (MPa)	Max. strain (%)	Yield strength (MPa)	Ultimate strength (MPa)	Max. strain (%)
Mg-1.2Zn-0.5Ca	As-cast	50.6 ± 6.1	60.9 ± 10.5	260.2 ± 5.9	18.1 ± 0.7	59.7 ± 4.2	120.6 ± 4.7	3.2 ± 0.2
	Heat-treated	61.4 ± 2.8	118.8 ± 12.7	306.5 ± 7.3	19.8 ± 1.3	83.1 ± 6.4	150.8 ± 7.3	4.7 ± 0.3
Mg-1.2Zn-0.5Ca-0.5Mn	As-cast	51.6 ± 3.6	71.7 ± 5.3	304.1 ± 8.2	28.9 ± 0.8	63.4 ± 3.5	125.1 ± 6.1	4.4 ± 0.1
	Heat-treated	62.9 ± 4.7	122.8 ± 9.4	352.8 ± 24.1	25.63 ± 2.2	88.9 ± 5.2	158.0 ± 8.4	4.8 ± 0.2

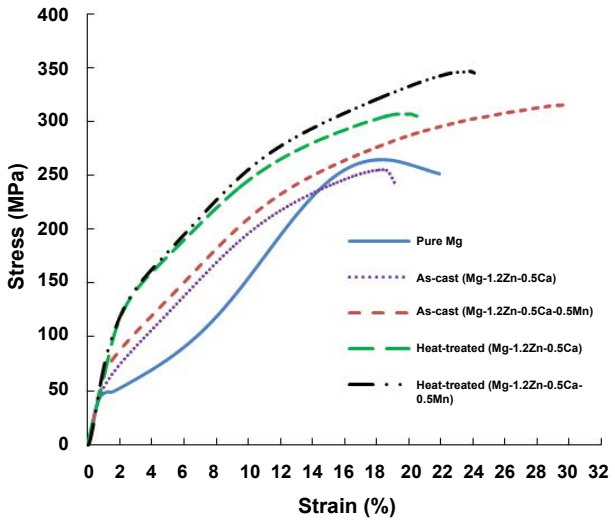

Figure 4: Compression stress-strain diagram of the Mg-1.2Zn-0.5Ca and Mg-1.2Zn-0.5Ca-0.5Mn alloys, as-cast and heat-treated.

Instruments Potentiostat was used to perform the PDP test in SBF at pH 7.4, 37 ± 1 °C and a constant scan rate of 1 mV/sec. Standard three-electrode system was used with silver chloride (Ag/AgCl) as the reference electrode, graphite rod as the counter electrode, and the sample as the working electrode.

Results and Discussion

Microstructure investigations

The optical micrographs of the as-cast Mg-1.2Zn-0.5Ca alloy in comparison to the Mg-1.2Zn-0.5Ca-0.5Mn alloy are shown in figure 1a and figure 1b, respectively. It can be seen that for both alloys, the secondary phase is uniformly distributed as lamellar eutectoids along the grain boundaries and as spherical eutectoids throughout the α-Mg matrix phase. More importantly, the grain size of the alloy after the addition of Mn was much lower than that for the Mn-free alloy. The average grain size of the Mg-1.2Zn-0.5Ca alloy and the Mg-1.2Zn-0.5Ca-0.5Mn alloy was around 216 μm and 67 μm, respectively. Such grain refinement effect is expected to result in an improved mechanical and corrosion properties for the Mg alloy [2,46]. For some other Mg-Zn-Ca-based alloys such as the as-cast ZX51 (Mg-5.25 wt.% Zn-0.6 wt.% Ca), the addition of Mn showed a negligible effect on the grain size [47]. However, it was reported in several recent studies that the addition of Mn plays a significant role in the grain refinement of the as-cast Mg-Zn-Ca-based alloys [22,40]. The decrease in the grain size is suggested to be due to the formation of constitutional under cooling in a diffusion layer that limits the growth stage [22].

Figure 2 shows the SEM observation of the as-cast Mg-1.2Zn-0.5Ca alloy (Figure 2a and Figure 2c) and the as-cast Mg-1.2Zn-0.5Ca-0.5Mn alloy (Figure 2b and figure 2d). The results of the SEM investigation supported the concluded findings of the optical micrographs. The microstructure of the ternary Mg-1.2Zn-0.5Ca alloy and the quaternary Mg-1.2Zn-0.5Ca-0.5Mn alloy shows the formation of the secondary phase at the grain boundaries and through the primary α-Mg matrix phase. The corresponding EDS analysis for both alloys confirms that the light areas with high concentrations of Zn and Ca (points 2 and 4 in Figure 2) are related to the $Ca_2Mg_6Zn_3$ eutectic phase. The EDS analysis for point 3 through the α-Mg matrix of the Mg-1.2Zn-0.5Ca-0.5Mn alloy (Figure 2d) showed traces of Mn, while no traces of Mn were found for the Mg-1.2Zn-0.5Ca alloy (point 1 and 2 of Figure 2c).

The SEM investigation of both alloys after the heat treatment process is shown in figure 3. It can be seen that the heat treatment process resulted in a more uniform size and shape of grains for both alloys. In addition, most of the white regions representing the secondary phase ($Ca_2Mg_6Zn_3$) between grain boundaries or throughout the grains vanished. This confirms that the heat treatment process resulted in a uniform distribution of the secondary phase ($Ca_2Mg_6Zn_3$) into finely-dispersed precipitates throughout the α-Mg matrix. Mechanical properties figure 4 shows the compression stress-strain diagram of the as-cast and heat-treated alloys in comparison to commercially pure Mg. It can be observed that the as-cast Mg-1.2Zn-0.5Ca-0.5Mn alloy has better

mechanical properties compared to the as-cast Mg-1.2Zn-0.5Ca alloy, this enhancement is represented in the higher strength and ductility of the Mg-1.2Zn-0.5Ca-0.5Mn alloy, which can be attributed the significant grain refinement after the addition of Mn. Moreover, the heat treatment response of the Mg-1.2Zn-0.5Ca-0.5Mn alloy was higher than that for the Mg-1.2Zn-0.5Ca alloy. For example, the compression yield strength and ultimate strength of the heat-treated Mg-1.2Zn-0.5Ca-0.5Mn were 122.8 MPa and 352.8 MPa, respectively. While, the compression yield strength and ultimate strength of the Mg-1.2Zn-0.5Ca alloy after the heat treatment were 118.8 MPa and 306.5 MPa, respectively. Also, it can be observed that the enhancement in the alloys' strength after the heat treatment process did not result in a significant change in the alloy's modulus of elasticity. The enhancement in the mechanical properties of both alloys after heat treatment is attributed to the uniform distribution of the finely-dispersed $Ca_2Mg_6Zn_3$ precipitates and hence, the formation of ordered monolayer G.P. zones [27].

Similar results were obtained from the tensile and the microhardness tests. Table 1 summarized the obtained mechanical properties for the as-cast and heat-treated alloys. The tensile strength and hardness increased significantly for both alloys after the heat treatment process. For instance, the tensile strength and hardness of the Mg-1.2Zn-0.5Ca-0.5Mn alloy increased from 125.1 MPa and 51.6 HV, for the as-cast alloy, to reach 158 MPa and 62.9 HV, respectively.

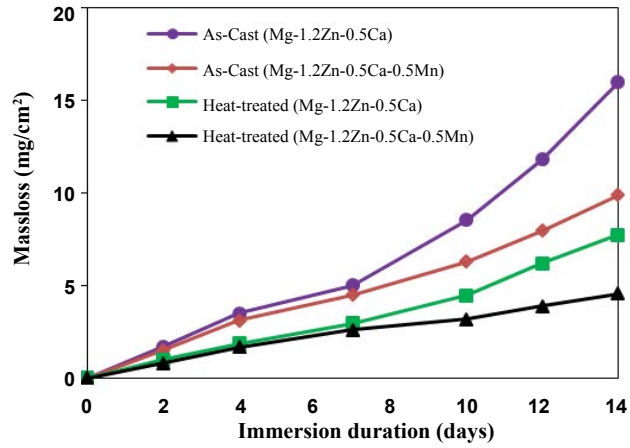

Figure 5: Mass loss obtained after the immersion of the as-cast and heat-treated Mg-1.2Zn-0.5Ca and Mg-1.2Zn-0.5Ca-0.5Mn alloy samples in SBF solution at 7.4 pH and 37 °C for 14 days.

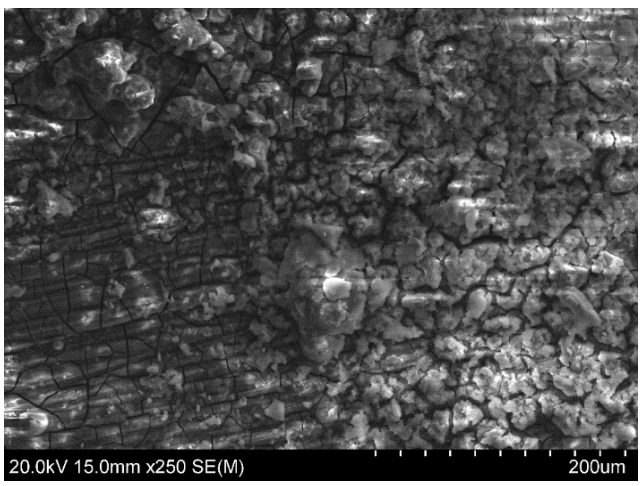

Figure 6: SEM micrograph of the corroded surface of the heat-treated Mg-1.2Zn-0.5Ca-0.5Mn alloy after immersion in SBF at 7.3-7.8 pH at 37 °C.

Immersion test

Figure 5 shows the mass loss of the as-cast and heat-treated alloy samples after immersion in SBF at pH 7.3-7.8 and 37 °C. The as-cast alloys showed fast *in vitro* corrosion rates, while the heat-treated alloys showed significantly lower corrosion rates. For example, the mass loss of the as-cast Mg-1.2Zn-0.5Ca-0.5Mn alloy increased 1.53 mg/cm² at day 3 to 9.9 by day 14 of immersion. This confirms that the superior corrosion resistance of the heat-treated alloys in compared to the as-cast alloys. The enhancement in the corrosion properties of the Mg-Zn-Ca-based alloys after heat treatment can be justified by the uniform distribution of the secondary phases into fine precipitates after the heat treatment process. The absence of the relatively large secondary phase areas from the microstructure after the heat treatment significantly reduced the galvanic corrosion of Mg leading to a slower corrosion rate [2,26]. If the Mg-1.2Zn-0.5Ca-0.5Mn alloy is to be compared with the Mg-1.2Zn-0.5Ca alloy, it can be easily seen that both the as-cast and heat-treated samples of the Mg-1.2Zn-0.5Ca-0.5Mn alloy showed lower corrosion rates than the Mn-free alloy. This is mainly attributed to the role of Mn in grain refinement and eliminating the harmful effect of impurities in the alloy [2].

Figure 6 shows the SEM investigation of the corroded surface of the heat-treated Mg-1.2Ca-0.5Ca-0.5Mn alloy after 7 days of the *in vitro* immersion test. The surface morphology shows corrosion product agglomerations on the surface. The EDS analysis of these corrosion products showed that the corrosion products on the surface are mainly formed of P, Na, Cl and S elements.

Electrochemical measurements

The electrochemical corrosion testing of the heat-treated alloys using the potentiodynamic polarization test showed similar results. Figure 7 shows the polarization curves for the heat-treated Mg-1.2Zn-0.5Ca and Mg-1.2Zn-0.5Ca-0.5Mn alloy samples tested in SBF at pH 7.4 and 37 °C. The heat-treated Mg-1.2Zn-0.5Ca-0.5Mn alloy showed more noble electrochemical corrosion characteristics (*i.e.,* less negative potential and lower current density) compared to the heat-treated Mn-free alloy. For example, the current density and corrosion potential of the Mg-1.2Zn-0.5Ca-0.5Mn alloy of -1.74 V and 410 μA/cm² respectively were better than those for the heat-treated Mg-1.2Zn-0.5Ca alloy -1.78 V and 680 μA/cm². Such electrochemical corrosion characteristics confirm that the heat-treated Mg-1.2Zn-0.5Ca-0.5Mn alloy possess the highest corrosion resistance.

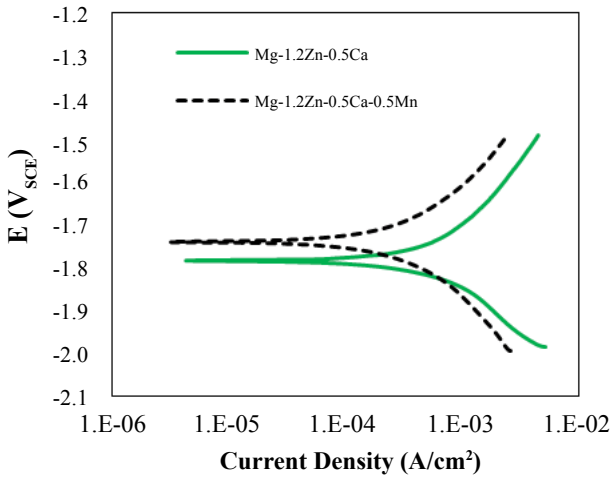

Figure 7: Potentiodynamic polarization curves for the heat-treated Mg-1.2Zn-0.5Ca and Mg-1.2Zn-0.5Ca-0.5Mn Alloys following placement in the SBF at 7.4 pH and 37 °C.

Conclusion

The addition of 0.5 wt.% Mn to the Mg-1.2Zn-0.5Ca alloy resulted in a significant grain refinement for the alloy by decreasing the grain size. In addition, the heat treatment of the Mg-1.2Zn-0.5Ca and the Mg-1.2Zn-0.5Ca-0.5Mn alloys resulted in a refinement and uniform distribution of the $Ca_2Mg_6Zn_3$ secondary phase into fine precipitates, which was confirmed by the SEM investigations. Mechanical properties and corrosion properties of the Mg-1.2Zn-0.5Ca and the Mg-1.2Zn-0.5Ca-0.5Mn alloys significantly increased after the heat treatment process due to the beneficial change in the microstructure. The best mechanical and *in vitro* corrosion properties were found for the heat-treated Mg-1.2Zn-0.5Ca-0.5Mn alloy. It can be concluded that in addition to its role in improving the mechanical properties, the addition of Mn to the Mg-1.2Zn-0.5Ca alloy was found to significantly improve the corrosion characteristics after heat treatment. Such heat-treated Mg-1.2Zn-0.5Ca-0.5Mn alloy can be coated with biocompatible coating for further control of its corrosion rate as a potential candidate for bone fixation applications.

Acknowledgment

The authors would like to acknowledge the financial support of the University of Toledo College of Medicine as a student fellowship for the first author as well as Ohio Third Frontier Technology Validation and Startup Fund. Also, the authors would like to thank Dr. Luo and and Dr. Poorganji for their continuous help.

References

1. Andani MT, Shayesteh Moghaddam N, Haberland C, et al. (2014) Metals for bone implants. Part 1. Powder metallurgy and implant rendering. Acta Biomater 10: 4058-4070.
2. Hamdy I, Sajedeh Nasr Esfahani, Behrang Poorganjib, et al. (2017) Resorbable bone fixation alloys, forming, and post-fabrication treatments. Materials Science and Engineering: C 70: 870-888.
3. Manivasagam G, Suwas S (2014) Biodegradable Mg and Mg based alloys for biomedical implants. Materials Science and Technology 30: 515-520.
4. Gosain AK, Song L, Corrao MA, et al. (1998) Biomechanical evaluation of titanium, biodegradable plate and screw, and cyanoacrylate glue fixation systems in craniofacial surgery. Plast Reconstr Surg 101: 582-591.
5. Perren SM (2002) Evolution of the internal fixation of long bone fractures. The scientific basis of biological internal fixation: choosing a new balance between stability and biology. J Bone Joint Surg Br 84: 1093-1110.
6. Mehanny S, Mahmoud Farag, RM Rashad, et al. (2012) Fabrication and Characterization of Starch Based Bagasse Fiber Composite. American Society of Mechanical Engineers 3: 1345-1353.
7. Amerstorfer F, Fischerauer SF, Fischer L, et al. (2016) Long-term in vivo degradation behavior and near-implant distribution of resorbed elements for magnesium alloys WZ21 and ZX50. Acta Biomater 42: 440-450.
8. Moghaddam NS, Mohsen Taheri Andani, Amirhesam Amerinatanzi, et al. (2016) Metals for bone implants: safety, design, and efficacy. Biomanufacturing Reviews 1: 1.
9. Mostofi, S, Bonyadi Rad E, Wiltsche H, et al (2016) Effects of Corroded and Non-Corroded Biodegradable Mg and Mg Alloys on Viability, Morphology and Differentiation of MC3T3-E1 Cells Elicited by Direct Cell/Material Interaction. PloS one 11: e0159879.
10. Zhang Y, Xu J, Ruan YC, et al. (2016) Implant-derived magnesium induces local neuronal production of CGRP to improve bone-fracture healing in rats. Nat Med 22: 1160-1169.
11. Zhen Z, Luthringer B, Yang L, et al. (2016) Proteomic profile of mouse fibroblasts exposed to pure magnesium extract. Mater Sci Eng C Mater Biol Appl 69: 522-531.
12. Zhao D, Witte F, Lu F, et al. (2017) Current status on clinical applications of magnesium-based orthopaedic implants: A review from clinical translational perspective. Biomaterials 112: 287-302.
13. Chen Y, Xu Z, Smith C, et al. (2014) Recent advances on the development of magnesium alloys for biodegradable implants. Acta biomaterialia 10: 4561-4573.
14. Joelle H, Elisabeth M, Annelie M, et al. (2015) Assessing the degradation performance of ultrahigh-purity magnesium in vitro and in vivo. Corrosion Science 91: 29-36.
15. Zijian L, Xunan Gua, Siquan Lou, et al. (2008) The development of binary Mg-Ca alloys for use as biodegradable materials within bone. Biomaterials 29: 1329-1344.
16. Yizao W, Guangyao X, Honglin L, et al. (2008) Preparation and characterization of a new biomedical magnesium-calcium alloy. Materials & Design 29: 2034-2037.
17. Zhang S, Zhang X, Zhao C, et al. (2010) Research on an Mg-Zn alloy as a degradable biomaterial. Acta Biomater 6: 626-640.
18. Berglund IS, Brar HS, Dolgova N, et al. (2012) Synthesis and characterization of Mg-Ca-Sr alloys for biodegradable orthopedic implant applications. J Biomed Mater Res B Appl Biomater 100: 1524-1534.
19. Harpreet S Brar, Joey Wong, Michele V Manuel (2012) Investigation of the mechanical and degradation properties of Mg-Sr and Mg-Zn-Sr alloys for use as potential biodegradable implant materials. Journal of the mechanical behavior of biomedical materials 7: 87-95.
20. Hamid R B R, Mohd Hasbullah Idris, Mohammed Rafiq Abdul Kadir, et al. (2012) Characterization and corrosion behavior of biodegradable Mg-Ca and Mg-Ca-Zn implant alloys. Applied Mechanics and Materials 121: 568-572.
21. Xiaobo Z, Guangyin Y, Lin M, et al. (2012) Biocorrosion properties of as-extruded Mg-Nd-Zn-Zr alloy compared with commercial AZ31 and WE43 alloys. Materials Letters 66: 209-211.
22. Bakhsheshi RH, Idris MH, Abdul-Kadir MR, et al. (2014) Mechanical and bio-corrosion properties of quaternary Mg-Ca-Mn-Zn alloys compared with binary Mg-Ca alloys. Materials & Design 53: 283-292.
23. Luckey T, B Venugopal (1977) Metal toxicity in mammals. Volume 1: Physiologic and chemical basis for metal toxicity. Plenum Press, New York.
24. Domingo JL (1995) Reproductive and developmental toxicity of aluminum: a review. Neurotoxicol Teratol 17: 515-521.
25. Flaten TP (2001) Aluminium as a risk factor in Alzheimer's disease, with emphasis on drinking water. Brain Res Bull 55: 187-196.
26. Ibrahim H, Andrew D Klarner, Behrang Poorganji, et al. (2016) The Effect of Heat-Treatment on Mechanical, Microstructural, and Corrosion Characteristics of a Magnesium Alloy With Potential Application in Resorbable Bone Fixation Hardware. American Society of Mechanical Engineers.
27. Oh-Ishi K, R Watanabeb, CL Mendis, et al. (2009) Age-hardening response of Mg-0.3 at.% Ca alloys with different Zn contents. Materials Science and Engineering: A 526: 177-184.
28. Sun Y, Baoping Zhang, Yin Wang, et al. (2012) Preparation and characterization of a new biomedical Mg-Zn-Ca alloy. Materials & Design 34: 58-64.
29. Cha PR, Han HS, Yang GF, et al. (2013) Biodegradability engineering of biodegradable Mg alloys: Tailoring the electrochemical properties and microstructure of constituent phases. Sci Rep 3.
30. Kirkland NT, Staiger MP, Nisbet D, et al. (2011) Performance-driven design of Biocompatible Mg alloys. JOM 63: 28-34.
31. Kirkland NT, N Birbilis (2014) Magnesium Biomaterials: Design, Testing, and Best Practice. Springer.
32. Nie J, B Muddle (1997). Precipitation hardening of Mg-Ca (-Zn) alloys. Scripta Materialia 37: 1475-1481.
33. Bettles C, MA Gibson, K Venkatesan, et al. (2004) Enhanced age-hardening behaviour in Mg-4 wt.% Zn micro-alloyed with Ca. Scripta Materialia 51: 193-197.
34. Gao X, SM Zhu, BC Muddle, et al. (2005) Precipitation-hardened Mg-Ca-Zn alloys with superior creep resistance. Scripta Materialia 53: 1321-1326.
35. Oh J, T Ohkubo, T Mukai, et al. (2005) TEM and 3DAP characterization of an age-hardened Mg-Ca-Zn alloy. Scripta Materialia 53: 675-679.
36. Ibrahim H, Klarner AD, Poorganji B, et al. (2017) Microstructural, Mechanical and Corrosion Characteristics of Heat-Treated Mg-1.2 Zn-0.5 Ca (wt.%) Alloy for Use as Resorbable Bone Fixation Material. J Mech Behav Biomed Mater 69: 203-212.
37. Spierings AB, Dawsonb K, Heelingc T, et al. (2017) Microstructural features of Sc-and Zr-modified Al-Mg alloys processed by selective laser melting. Materials & Design 115: 52-63.
38. Lu Y, Bradshaw AR, Chiu YL, et al. (2015) Effects of secondary phase and grain size on the corrosion of biodegradable Mg-Zn-Ca alloys. Materials Science and Engineering: C 48: 480-486.
39. Jeong-Hui Ji,1 Il-Song Park, Yu-Kyoung Kim, et al. (2015) Influence of Heat Treatment on Biocorrosion and Hemocompatibility of Biodegradable Mg-35Zn-3Ca Alloy. Advances in Materials Science and Engineering.

40. Yandong, Y, Kuang Shuzhen, Pei Teng, et al. (2015) Effects of Mn Addition on the Microstructure and Mechanical Properties of As-cast and Heat-Treated Mg-Zn-Ca Bio-magnesium Alloy. Metallography, Microstructure, and Analysis 4: 381-391.

41. Boehlert C, Knittel K (2006) The microstructure, tensile properties, and creep behavior of Mg-Zn alloys containing 0-4.4 wt.% Zn. Materials Science and Engineering: A 417: 315-321.

42. Bakhsheshi-Rad HR, Abdul-Kadirb MR, Idrisa MH, et al. (2012) Relationship between the corrosion behavior and the thermal characteristics and microstructure of Mg-0.5 Ca-xZn alloys. Corrosion Science 64: 184-197.

43. Daniela Z, Naemi A Zumdick (2015) Influence of Ca and Zn on the microstructure and corrosion of biodegradable Mg-Ca-Zn alloys. Corrosion Science 93: 222-233.

44. Oyane A, Kim HM, Furuya T, et al. (2003) Preparation and assessment of revised simulated body fluids. J Biomed Mater Res A 65: 188-195.

45. Lokesh C, RK Singh Raman (2013) Mechanical integrity of magnesium alloys in a physiological environment: Slow strain rate testing based study. Engineering Fracture Mechanics 103: 94-102.

46. Erlin Z, Dongsong Y, Liping Xu, et al. (2009) Microstructure, mechanical and corrosion properties and biocompatibility of Mg-Zn-Mn alloys for biomedical application. Materials Science and Engineering: C 29: 987-993.

47. Tonga LB, Zhenga MY, Xub SW, et al. (2011) Effect of Mn addition on microstructure, texture and mechanical properties of Mg-Zn-Ca alloy. Materials Science and Engineering: A 528: 3741-3747.

DOI: 10.36959/508/392 | Volume 1 | Issue 1